Surface electronic structure of Si(001)2×2-In studied by angle-resolved photoelectron spectroscopy

H. W. Yeom
Department of Physics, Faculty of Science, Tohoku University, Sendai 980-77, Japan

T. Abukawa, Y. Takakuwa, Y. Mori, and T. Shimatani
Research Institute for Scientific Measurements, Tohoku University, Sendai 980-77, Japan

A. Kakizaki
Synchrotron Radiation Laboratory, ISSP, The University of Tokyo, Tokyo 106, Japan

S. Kono
Research Institute for Scientific Measurements, Tohoku University, Sendai 980-77, Japan
(Received 31 August 1995; revised manuscript received 23 October 1995)

Angle-resolved photoelectron spectroscopy (ARPES) using synchrotron radiation was employed to study the electronic structure of a well-ordered single-domain Si(001)2×2-In surface. The existence of five surface state bands, denoted as S_1, S_2, S_2', S_3, and S_3' is revealed within the bulk band gap between 0.6 and 2.2 eV in binding energy (E_B). The dispersions of these surface states are determined for most of the symmetry axes in the 2×2 surface Brillouin zone (SBZ), which turn out to be essentially identical to those observed for Si(001) 2×2-Al recently [Surf. Sci. Lett. **321**, L177 (1994)]. Symmetries of the surface states with respect to two mirror axes of the SBZ are determined by the polarization dependence of ARPES intensities. A comparison to a theoretical calculation makes it possible to determine that the smallest E_B state S_1 is due to the In dimer bond and S_2, S_2', S_3, and S_3' are due to bonds between In dimers and topmost Si atoms, and that the In dimers are parallel to the substrate Si dimers. Besides these five surface state bands, two other spectral features are observed within the bulk band gap, which can be related to similar features observed for a clean Si(001) surface.

I. INTRODUCTION

During the last decade, the electronic structures of adsorbed Si(001) surfaces have been one of the most extensively pursued topics in surface science.[1] Throughout various adsorbates such as group-I (H, Na, K, and Cs), -III (Al, Ga, and In), -IV (Si and Ge), and -V (As, Sb, and Bi) elements, the most commonly observed surface structure has been the dimer structures of adsorbate and/or substrate Si.[1,2] The properties of a few surface states (SS's) for some dimer-structure Si(001) surfaces have been well understood hitherto. Examples of them are lone-pair SS's found for the adsorption of group-V element of As,[1,3] and SS's due to saturated dangling bonds for the adsorptions of K and Na.[1,4,5] However, much is not known for SS's of other adsorbed Si(001) surfaces; thus the identification and characterization of SS's remains for these interesting surfaces.

In this respect, the electronic structures of several ordered phases due to group-III metal adsorption on Si(001) deserve to be noted. The adsorption of group-III metals has been reported to result in unique surface structures: dimerized adsorbate metal overlayers on a still-dimerized Si substrate.[6,22] Several surface phases composed of long-range-ordered dimer arrays such as 2×3, 2×5, and the frequently encountered 2×2 phases, have been observed at different metal coverages—0.3, ~0.4, and 0.5 ML, respectively—for Al,[9,10,21] Ga,[6,8,11] and In (Refs. 7 and 21) adsorptions. The orientation of the adsorbate metal dimers with respect to the substrate Si dimers, especially for the 2×2 phase, has been the aim of various theoretical[12–14,18,20] and experimental studies. Most of the studies have favored the parallel dimer structure, where the metal dimers are parallel to the Si dimers.[12–18,20,22] This surface structure is in sharp contrast to the well-known dimer structure due to adsorption of group-V elements which form orthogonal dimers with 1×2 long-range order at 1 ML.[1,3]

However, in contrast to the large amount of structural studies on these surfaces, there have been only a few electronic structure studies. Northrup *et al.*[12] reported an *ab initio* band calculation and an angle-resolved photoemission spectroscopy (ARPES) measurement for SS bands along the [010] axis of a double-domain (DD) Si(001)2×2-In surface. They identified three SS's at E_B of 0.8–2 eV, and suggested they are back-bond SS's of the adsorbate dimers. Enta, Suzuki, and Kano[11] observed several SS's at similar E_B along [110] and $[\bar{1}10]$ axes of a single-domain (SD) Si(001) 2×2-Ga surface by ARPES. On the other hand, in a recent scanning-tunneling-microscopy (STM) study on Si(001) 2×2-Al, the result was interpreted to give evidence of Al-Si back bonds present at an E_B of ~3 eV.[17] Very recently we performed detailed ARPES measurements using synchrotron radiation on a SD Si(001)2×2-Al surface, and were able to resolve five SS bands related to the 2×2 phase at 0.8–2.1 eV in E_B.[23] We suggested that these five SS's correspond to the one dimer and four back-bond SS's due to adsorbed Al

 © 1996 The American Physical Society

dimers,[23] and, thus, questioned the previous suggestion on the origin of SS's.[12,17]

In this paper, we extend our previous work on the Si(001) 2×2-Al surface to a similar surface of well-ordered SD Si(001)2×2-In. Employing ARPES using linearly polarized synchrotron radiation, we investigated the existence, dispersions, and symmetry properties of SS's along most of the symmetry axes in the surface Brillouin zone (SBZ) in detail. Inside of the bulk band gap, are five SS's identified, whose dispersions follow the symmetry of the 2×2 SBZ. This result reinforces the previous ARPES result for the Si(001)2×2-Al surface.[23] A comparison to a recent theoretical calculation[20] made it possible to assign the origins of SS bands: the smallest-E_B state as the In dimer-bond and others as the four back bonds between the In dimer and substrate Si. In addition, this comparison provides corroborating evidence for the parallel dimer structure.[10,12,15] The detailed characteristics of the five SS bands and other spectral features within the bulk band gap are discussed in comparison to the results of existing experimental and theoretical studies.

II. EXPERIMENTAL DETAILS

ARPES measurements using synchrotron radiation were performed with a commercial spectrometer on the beam line BL-18A of the Institute for Solid State Physics at the Photon Factory, National Laboratory for High Energy Physics in Tsukuba, Japan.[4,23] The beam line delivers photon beams in the energy range 10–150 eV with a constant-deviation-angle grazing-incidence monochromator. The overall angular and energy resolutions were ~1° and ~140 meV, respectively, at photon energies ($h\nu$'s) of 21.2 and 18.6 eV. The base pressure of the spectrometer was $\sim 1.5\times 10^{-11}$ mbar during the experiment.

A mirror-polished Si wafer ($25\times 3.5\times 0.38$ mm^3) was used as a substrate. The Si wafer was heated by direct resistive heating, and its temperature was monitored by an optical pyrometer. A wide-terrace SD Si(001)2×1 surface was prepared by preoxidation[24] and cycles of *in situ* annealing and Si deposition.[4] The fraction of minor domain (1×2) was below 10%, as determined from the intensity ratio of low-energy-electron-diffraction (LEED) spots for the two domains. Indium was deposited onto the SD Si(001)2×1 surface held at room temperature (RT) from a Knudsen cell. The cell was thoroughly degassed to maintain the pressure during deposition below $\sim 1.0\times 10^{-10}$ mbar. The amount of deposited In on the RT substrate was determined by the x-ray photoelectron spectroscopy (XPS) intensity ratio of In 3d to Si 2p, which was calibrated by a quartz thickness monitor.[21] A well-ordered SD 2×2 phase was formed by 0.5-ML In deposition without any annealing.[21] No trace of contaminants was found by XPS before and after a deposition. A LEED pattern for this phase is shown in Fig. 1(a). A very good SD property of this phase has been proved by an x-ray photoelectron diffraction study.[22] The corresponding structural model, the parallel dimer model, is depicted schematically in Fig. 1(b), for which clear experimental evidence has recently been given.[22] This SD phase on a wide-terrace substrate would prevent possible artifacts on spectroscopic measurements, which may be the case for the usual DD samples due to higher step densities.

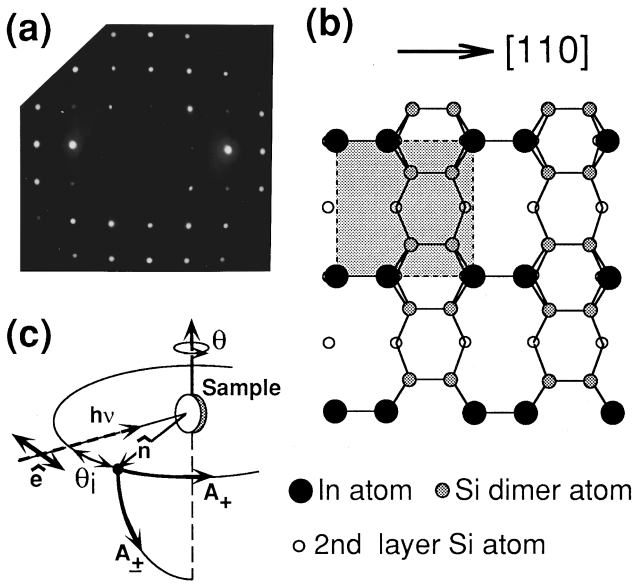

FIG. 1. (a) LEED pattern at an electron-beam energy of 90 eV for a single-domain Si(001)2×2-In surface and (b) a structural model, the parallel dimer model, for it. The surface unit cell is depicted by the dashed line and shadowing in it. (c) A schematic illustration of the two data-taking geometries A_+ and $A_\pm$ an explanation for which is given in the text.

ARPES spectra were measured at a step of 2° along various symmetric axes of the 2×2 surface Brillouin zone [SBZ; see Fig. 4(h)]. We measured ARPES spectra not only along symmetric axes including the origin $\bar{\Gamma}_{00}$, like [110], [$\bar{1}$10], and [010], but also along symmetric axes excluding the origin, such as $\bar{\Gamma}_{10}$-$\bar{\Gamma}_{11}$, $\bar{\Gamma}_{01}$-$\bar{\Gamma}_{11}$, $\bar{J}'_{00}$-$\bar{J}'_{10}$, and $\bar{J}_{00}$-$\bar{J}_{01}$, for a complete determination of SS dispersions. To scan the latter SBZ lines, the direction of photoelectron detection was varied in both polar (θ_e) and azimuthal angles in such a way that the surface parallel component of the electron wave vector ($k_\parallel$) at $E_B = 1.5$ eV lies on an aimed symmetric line. The angular step in these scans was then adjusted to result in $k_\parallel$ steps of one-tenth or sometimes one-twentieth of the separation of $\bar{\Gamma}$-$\bar{\Gamma}$. The measurements along the axes including $\bar{\Gamma}_{11}$ instead of $\bar{\Gamma}_{00}$ may be helpful to determine the dispersions of SS's for two reasons. First, for the Si(001) surface the bulk band gap is much wider around $\bar{\Gamma}_{11}$ than $\bar{\Gamma}_{00}$, thus the SS's can be found more clearly around $\bar{\Gamma}_{11}$. Second, a SS with a weak intensity around $\bar{\Gamma}_{00}$ may appear dominantly around $\bar{\Gamma}_{11}$ due to the matrix element effect. These benefits have indeed been proved successful for several surfaces.[4,5,23,25] ARPES spectra presented were taken with linearly polarized synchrotron radiation of 21.2 and 18.6 eV. The Fermi level (E_F) was determined from that of a Ta clip which holds the Si sample.

In order to determine the symmetries of a SS with respect to the mirror axes of the SBZ, namely [110] and [$\bar{1}$10], two different measurement geometries, denoted as A and $A_\pm$, are used [Fig. 1(c)]. In the former geometry A_+, the photoelectron emission always lies in the plane defined by the surface normal ($\hat{n}$) of the sample, and the incident light whose polar angle from surface normal (θ_i) is fixed at 45°. Since the linear-polarization vector ($\hat{e}$) of incident synchrotron radia-

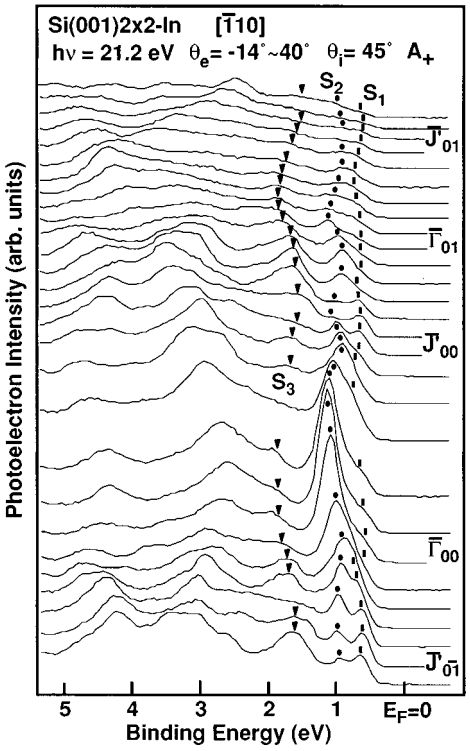

FIG. 2. ARPES spectra for a single-domain Si(001)2×2-In surface taken along [$\bar{1}$10] in the A_+ geometry with a synchrotron radiation of $h\nu$=21.2 eV. The incidence angle of the photon with respect to the surface normal (θ_i) is 45°, and the angular step of emission angles (θ_e) between neighboring spectra is 2°. Each spectrum is normalized by the incident photon flux. The corresponding surface Brillouin-zone position is specified approximately by the symmetry symbols [cf. Fig. 4(h)]. The peak positions for different assigned surface-state bands are marked with different symbols.

tion is always in the plane of emission in this geometry, only the electronic states with even symmetry are excited for a scan along a mirror axis. On the other hand, in the latter geometry $A_\pm$, the emission is kept in the plane which contains $\hat{n}$ and is perpendicular to the plane defined for A_+ geometry. If θ_i is zero in this geometry, $\hat{e}$ is always orthogonal to the plane of emission; thus only the odd-symmetry states can be excited. However, since the actual measurement situation made this condition impossible, θ_i was fixed at 28° and both even- and odd-symmetry states are excited in the geometry $A_\pm$. Finally, through comparison of the spectra along a mirror-symmetric axis taken in these two different geometries, we can determine the symmetries of each SS. Along the other SBZ lines of [010], $\bar{\Gamma}_{10}$-$\bar{\Gamma}_{11}$, $\bar{\Gamma}_{01}$-$\bar{\Gamma}_{11}$, $\bar{J}'_{00}$-$\bar{J}'_{10}$, and $\bar{J}_{00}$-$\bar{J}_{01}$, SS's with both symmetries can contribute to the spectra in principle.

A special method is used for compiling a set of ARPES spectra measured along an axis of the SBZ as introduced above.[23,25] In brief, the second derivatives of normalized spectra with respect to E_B were taken after a proper smoothing process. Each of the differentiated spectra is converted to a grey-scale bar. The brightness in the bar is roughly proportional to I/W, where I is the intensity of a peak above smooth background, and W is the width. The grey-scale bars of a set of ARPES spectra were gathered together into a grey-scale E_B-$k_\parallel$ diagram, where the abscissa is $k_\parallel$ and the ordinate is E_B. In this way, one can easily see not only the dispersive behaviors of peaks but also the evolutions in their intensities and widths in $k_\parallel$ space.

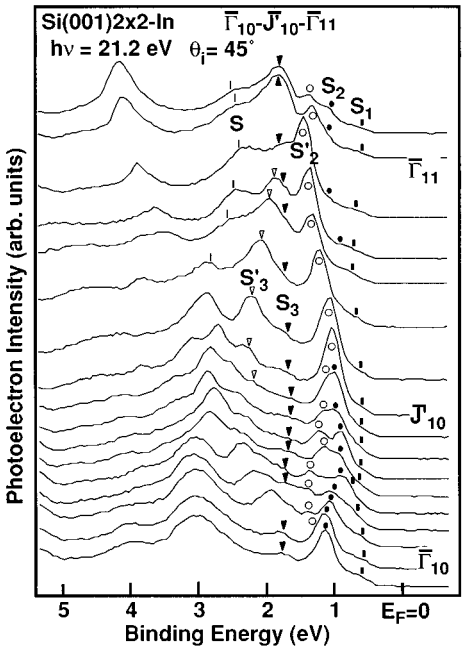

FIG. 3. Similar to Fig. 2, but along the symmetrically equivalent surface-Brillouin-zone line to the [$\bar{1}$10] axis, i.e., $\bar{\Gamma}_{10}$-$\bar{J}'_{10}$-$\bar{\Gamma}_{11}$. See the text for the detailed method of this scan.

III. ARPES RESULTS

In Figs. 2 and 3 we show the typical ARPES spectra taken along [$\bar{1}$10] and $\bar{\Gamma}_{10}$-$\bar{J}'_{10}$-$\bar{\Gamma}_{11}$ (symmetrically equivalent to [$\bar{1}$10]), respectively. All the spectra shown are normalized by the incident photon flux. The corresponding grey-scale E_B-$k_\parallel$ diagrams for the whole scans, along seven axes in total, are shown in Fig. 4, where features are shown in an E_B region from E_F to 2.5 eV in which the projected bulk band gaps are present. The white dashed lines in Fig. 4 represent the edges of the bulk band projected into the 1×1 SBZ. To determine the position of this bulk band edge with respect to E_F, the E_B's of bulk spectral features are compared to those of the previous ARPES on a clean Si(001) surface.[26] The bands depicted with black dashed lines in Fig. 4 are SS bands, and the assignments of these SS bands are done by taking into account the spectral features in Fig. 4 and the raw spectra as a whole as well as the dependences of spectra on $h\nu$, $\hat{e}$, and θ_i, as explained below.

In Fig. 2, we can see three bands denoted as S_1, S_2, and S_3 within 2 eV from E_F, whose peak positions are marked with filled squares, circles, and triangles, respectively. S_1 shows a small downward [downward (upward) means to larger E_B (to smaller E_B) throughout this paper] dispersion from $\bar{\Gamma}$, and has the smallest E_B among the three states. The second state S_2 disperses in the opposite direction from $\bar{\Gamma}$ with dominant intensity, and draws close to S_1 in the middle of $\bar{\Gamma}$-$\bar{J}'$. Another band S_3 can be found around ~1.8 eV, with broad width and rather large upward dispersion from $\bar{\Gamma}$ to $\bar{J}'$. The detailed dispersions for these three states can be

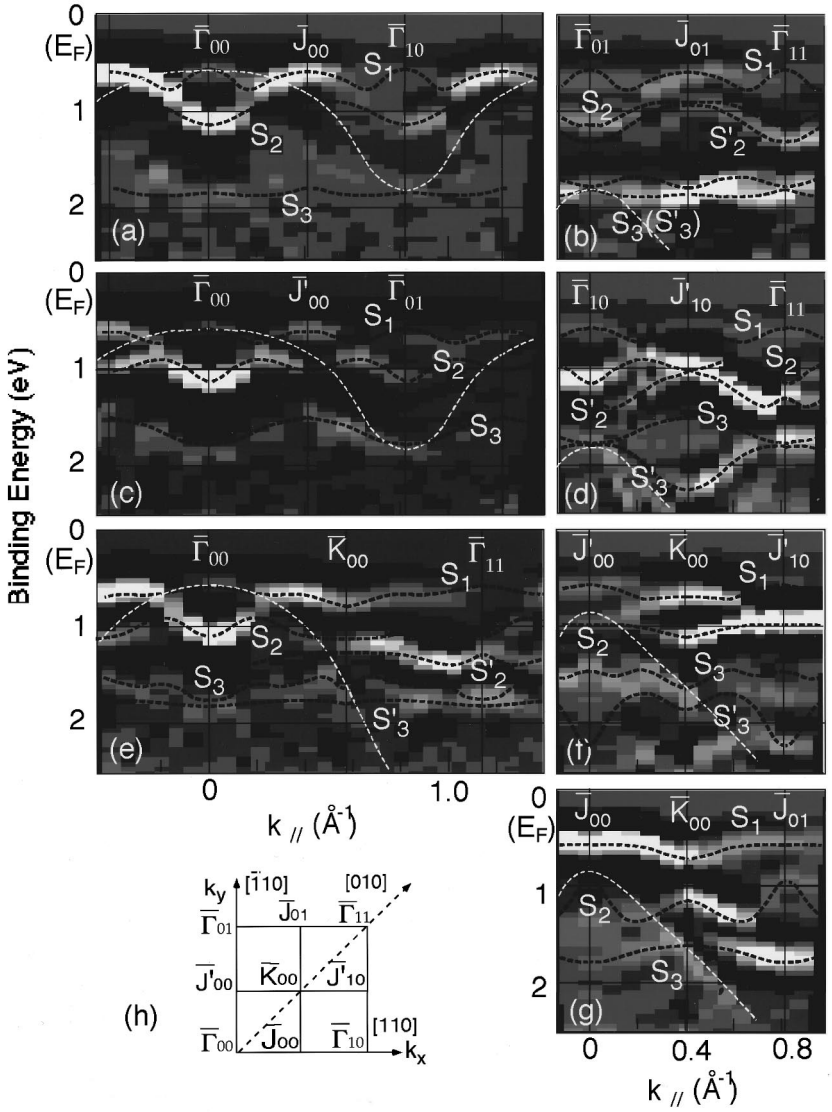

FIG. 4. (a)–(g) Grey-scale $E_B-k_\parallel$ diagrams for a Si(001)2×2-In surface taken from ARPES scans at $h\nu=21.2$ eV and $\theta_i=45°$ along the marked symmetric lines of the 2×2 surface Brillouin zone (SBZ). White broken lines are the edges of the bulk band projected into the 1×1 SBZ. The determined dispersions for the surface states are depicted with black dashed lines. (h) SBZ of a single-domain Si(001)2×2-In surface with symbols of relevant symmetric points. The "2*x*" direction of the substrate 2×1 is along [110] (k_x). Diagrams (a) and (b) [(c) and (d)] are for the symmetry-equivalent direction of $\bar{\Gamma}$-$\bar{J}$ ($\bar{\Gamma}$-$\bar{J}'$). A brief explanation of the grey-scale E_B-$k_\parallel$ diagram is made in the text.

deduced from the corresponding grey-scale E_B-$k_\parallel$ diagrams (just "diagram" hereafter) as depicted by black dashed lines in Fig. 4(c).

Along the other mirror axis [110], we can also find the three SS's, S_1, S_2, and S_3, as shown in Fig. 4(a). The dispersions of S_1 and S_2 along [110] are quite similar to those along [$\bar{1}$10], except for the dispersion of S_2 around J. Though it is not so easy to distinguish S_3 in the diagram due to its low intensity and broad peak shape, its dispersion was tentatively depicted in the figure through a close inspection of the diagram and raw spectra. This dispersion will be made clear below.

Along $\bar{\Gamma}_{10}$-$\bar{J}'_{10}$-$\bar{\Gamma}_{11}$, which is symmetrically equivalent to [$\bar{1}$10], we can find additional SS's other than S_1, S_2, and S_3, as shown in Figs. 3 and 4(d). Through the intensity of S_1 is very weak, its dispersion appears to be the same as that along [$\bar{1}$10]. However, S_2 splits into two branches from $\bar{\Gamma}_{10}$, and its second branch becomes dominant between $\bar{J}'_{10}$ and $\bar{\Gamma}_{11}$ (Fig. 3). The dispersion of the smaller E_B branch is the same as that of S_2 along [$\bar{1}$10]. Hence we denote the additional larger E_B branch as S'_2. These two split states look degenerate at $\bar{\Gamma}$ and J', and have a maximum separation of ~0.5 eV in the middle of $\bar{\Gamma}$-$\bar{J}'$. Here the meaning of degeneration is valid only within the experimental resolution. A similar splitting can also be found for S_3. In Fig. 3, S_3 splits into two states from $\bar{\Gamma}_{11}$: the additional larger E_B branch, called S'_3 has a large downward dispersion with dominant intensity over its smaller E_B branch S_3 which has a small upward dispersion toward J' in the same way as along [$\bar{1}$10]. Around $\bar{\Gamma}_{10}$, S_3 and S'_3 overlap with a spectral feature of the bulk band, as seen in Fig. 4(d).

Two similar branch structures for both S_2 and S_3 can be deduced not only along $\bar{\Gamma}$-$\bar{J}'$ but also along $\bar{\Gamma}$-$\bar{J}$ from the ARPES scan along $\bar{\Gamma}_{01}$-$\bar{J}_{01}$-$\bar{\Gamma}_{11}$, which is a direction symmetrically equivalent to [$\bar{1}$10]. As shown in Fig. 4(b), though the dispersion of S_1 can be assigned to be identical to that along [$\bar{1}$10] axis between $\bar{\Gamma}_{01}$ and $\bar{\Gamma}_{11}$, the dispersions of S_2 and S_3 appear to be slightly different from those along [$\bar{1}$10]. First, S_2 disperses to a slightly larger E_B between $\bar{\Gamma}_{01}$ and $\bar{J}_{01}$ to result in a ~0.15 eV larger E_B at $\bar{\Gamma}_{11}$ than $\bar{\Gamma}_{01}$. It is possible to assign two branches for S_2 as drawn in Fig. 4(b) (black dashed lines) to explain this dispersion from the fact that S_2 has a very clearly larger E_B branch along

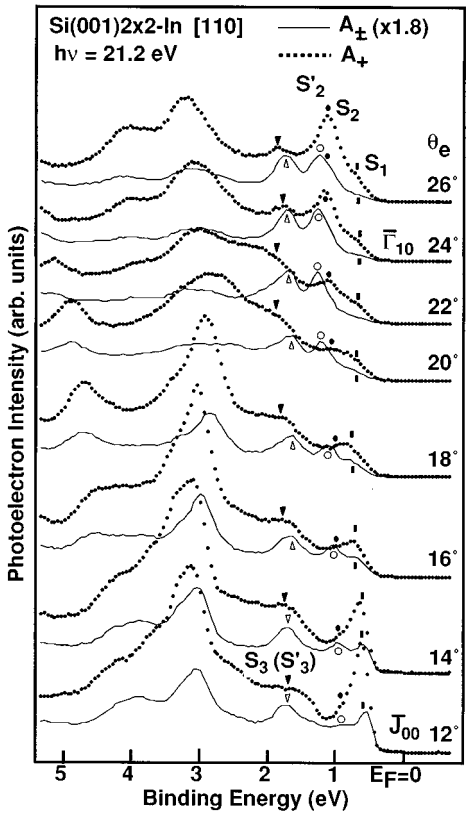

FIG. 5. Polarization-dependent ARPES spectra for a single-domain Si(001)2×2-In surface recorded with $h\nu=21.2$ eV along a mirror axis [110] from $\bar{J}_{00}$ to $\sim\bar{\Gamma}_{10}$ at two different geometries, A_+ (dots) and $A_\pm$ (solid lines) (see the inset of Fig. 9). The emission angles (θ_e) are given in the figure with the corresponding surface-Brillouin-zone positions. To compare the intensities for the two different geometries, the spectra at the $A_\pm$ geometry are normalized with the intensities of the background above E_F, that is, multiplied by 1.8. Different resolved surface-state bands are marked with different symbols.

$\bar{J}'_{10}$-$\bar{\Gamma}_{11}$ [Fig. 4(d)], and the fact that S_2 follows the 2×2 SBZ periodicity along other axes. Though not so well resolved, S_3 appears to have its branch at a slightly smaller E_B, as shown in Fig. 4(b). These two-branch structures of S_2 and S_3 along $\bar{\Gamma}$-$\bar{J}$ will be made much more clear if we consider the symmetries of the SS's through the $\hat{e}$ dependence of the spectra.

In order to characterize the symmetries of the five SS's observed, we studied the $\hat{e}$ dependence of ARPES spectra along the two mirror-symmetric SBZ axes [110] and [$\bar{1}$10], as shown in Fig. 5 for [110]. The spectra taken at $A_\pm$ geometry are normalized so as to make the intensity of the background above E_F the same as in the spectra taken at A_+ geometry. Since this background intensity is expected to have no dependence on $\hat{e}$, this normalization compensates for the effects of the geometrical change.

Between $\bar{J}_{00}$ and $\bar{\Gamma}_{10}$ (see Fig. 5), S_1 appears with much less intensity in $A_\pm$ (solid line) than A_+ geometry (dots) indicating that it has an even symmetry. In addition, two different states become dominant instead of S_2 and S_3 in $A_\pm$ geometry: one at slightly larger E_B than S_2 (open circles), and the other at slightly smaller E_B than S_3 (open triangles). These two states are definitely odd-symmetry states, while S_2 and S_3 are even. This behavior manifests itself in the two branch structure of S_2 and S_3 introduced in Fig. 4(b). The dispersions of these two odd states in $\bar{J}_{00}$-$\bar{\Gamma}_{10}$ are the same as those assigned for the additional branches between $\bar{J}_{01}$ and $\bar{\Gamma}_{11}$ in Fig. 4(b). *Thus the reality of the two branch structures of S_2 and S_3 is that two adjacent states with different symmetries exist.* Hence S'_2 and S'_3 appeared only in the scan along $\bar{\Gamma}_{01}$-$\bar{J}_{01}$-$\bar{\Gamma}_{11}$, which has no symmetry preference. Along the other mirror axis [$\bar{1}$10], the behaviors of S_1, S_2, and S'_2 for the change of $\hat{e}$ are almost the same as along [110], indicating that the symmetries of them along [$\bar{1}$10] are the same as along [110]: even for S_1 and S_2, and odd for S'_2. However, the symmetries of S_3 and S'_3 are not so clear along this axis due to their low intensities and broad widths, although it is tempting to assign S_3 and S'_3 with even and odd symmetries, respectively, from the appearance of S'_3 only along $\bar{\Gamma}_{10}$-$\bar{J}'_{10}$-$\bar{\Gamma}_{11}$.

Along [010] axis [see Fig. 4(e)], we can observe all five SS's identified above, because there is no symmetry preference in the scan along this non-mirror-symmetric axis. S_1 has a small dispersion and a low intensity around $\bar{\Gamma}$ as along the other axes. S_2 appears as two branches: at $k_\parallel$ less than $\bar{K}_{00}$, the smaller E_B branch is dominant while the larger E_B branch S'_2 can barely be distinguished, and vice versa at $k_\parallel$ greater than $\bar{K}_{00}$. The two possible branches of S_3 are not clearly resolved in Fig. 4(e), probably due to small splitting and wide widths. But we could clearly observe the two-branch structures of S_3, and S_2, through the change of their relative intensities with respect to θ_i: the splitting of the two branches is about 0.2 eV for both S_2 and S_3 at $\sim\bar{K}_{00}$. Considering these splittings, the dispersions of S_2 (S'_2) and S_3 (S'_3) can be deduced as in Fig. 4(e).

The dispersions of SS's along the two edges of the SBZ, $\bar{J}^r_{00}$-$\bar{K}_{00}$-$\bar{J}'_{10}$ and $\bar{J}_{00}$-$\bar{K}_{00}$-$\bar{J}_{01}$ were also determined through similar procedure as shown in Figs. 4(f) and 4(g). The traces of S'_2 (S'_3) were hardly found along both $\bar{J}_{00}$-$\bar{K}_{00}$-$\bar{J}_{01}$ and $\bar{J}'_{00}$-$\bar{K}_{00}$-$\bar{J}'_{10}$ (along $\bar{J}_{00}$-$\bar{K}_{00}$-$\bar{J}_{01}$).

As shown in Fig. 4, along the SBZ lines of $\bar{\Gamma}_{10}$-$\bar{\Gamma}_{11}$, $\bar{\Gamma}_{01}$-$\bar{\Gamma}_{11}$, $\bar{J}'_{00}$-$\bar{J}'_{10}$, and $\bar{J}_{00}$-$\bar{J}_{01}$, all excluding $\bar{\Gamma}_{00}$, the projected bulk-band gaps are very wide, and all five SS's lie well within the bulk band gaps. Furthermore, throughout all the SBZ lines measured, all five SS's can be assigned to follow the symmetry of the 2×2 SBZ in their dispersions, indicating that all these SS's are indeed the intrinsic SS's of the 2×2 phase induced by In adsorption. The assignment of SS's can be further confirmed by the $h\nu$ dependence of their E_B's and dispersions. Figure 6(a) compares the normal-emission spectra taken at $h\nu=21.2$ and 18.6 eV showing that the E_B's of S_1, S_2, and S_3 are invariant under the change of $h\nu$. We also measured ARPES spectra along $\bar{\Gamma}_{10}$-$\bar{J}'_{10}$ and $\bar{K}_{00}$-$\bar{J}'_{10}$ to check the $h\nu$ dependence of the detailed dispersions of the SS's assigned above. the results of this measurement are shown in Figs. 6(b) and 6(c), respectively, as diagrams which are to be compared with Figs. 4(d) and 4(f). It is evident in the figures that the dispersions of the SS's assigned above are invariant under the change of $h\nu$ from 21.2 to 18.6 eV, confirming the SS nature of the five states.

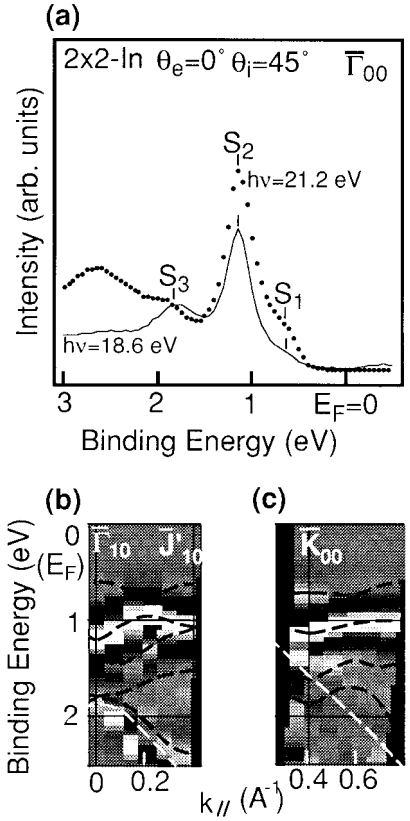

FIG. 6. (a) Normal-emission ($\bar{\Gamma}_{00}$) ARPES spectra for a Si(001) 2×2-In surface taken at two different photon energies: 21.2 (dots) and 18.6 eV (solid line). The incident angle of photon (θ_i) was fixed at 45°. (b) Grey-scale E_B-$k_\parallel$ diagrams for a single-domain Si(001)2×2-In surface taken from the ARPES scans at $h\nu=18.6$ eV and $\theta_i=45°$ along $\bar{\Gamma}_{10}$-$\bar{J}'_{10}$ of the 2×2 surface Brillouin zone. (c) Similar to (b) but along $\bar{K}_{00}$-$\bar{J}'_{10}$. The formats of (b) and (c) are the same as Figs. 4(a)–4(g).

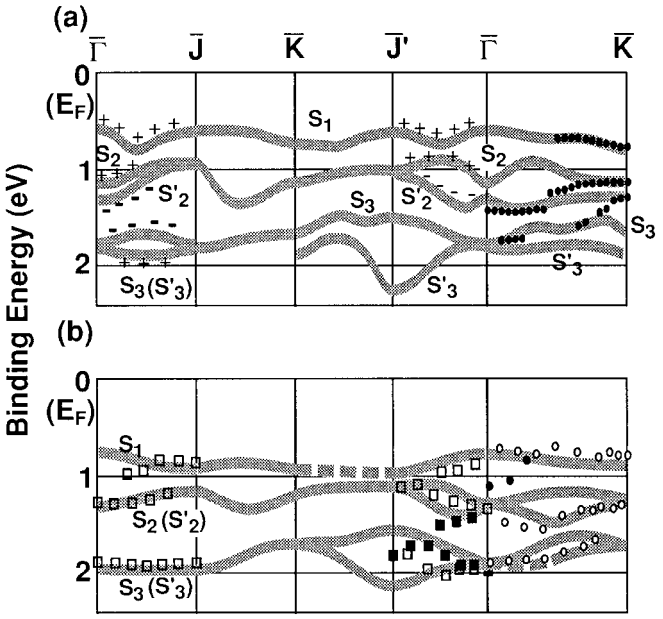

FIG. 7. Summary of the dispersions of the five surface states (SS's) assigned for (a) Si(001)2×2-In and (b) Si(001)2×2-Al (Ref. 23) surfaces for comparison. Parts of dispersions drawn with broken lines are tentative. The width of the lines for the dispersions roughly corresponds to the average experimental error in determining E_B of the SS's. For the case of Si(001)2×2-In in (a), the determined symmetries of the SS's are given with + and − symbols for even and odd symmetries, respectively. The dots in (a) represent the calculated SS dispersions for Si(001)2×2-In taken from Ref. 12. The previous results of the SS dispersions for Si(001)2×2-In (Ref. 12) and -Ga (Ref. 11) are also shown in (b) with circles and squares, respectively, for comparison. The open and closed symbols are taken from different parts of the SBZ (though symmetrically equivalent).

Figure 7(a) summarizes the dispersions of the five SS bands. The branches of S_2 and S_3 along $\bar{J}$-$\bar{K}$-$\bar{J}'$ and $\bar{J}$-$\bar{K}$, respectively, were not resolved. The determined symmetries for each SS along [110] and [$\bar{1}$10] are shown with + and − symbols for even and odd symmetries, respectively. It is evident that the 2×2 In surface is semiconducting with the highest occupied state at $E_B\sim0.6$ eV. S_2 and S'_2 seem to degenerate in $\bar{J}$-$\bar{K}$-$\bar{J}'$, and S_3 and S'_3 are not so well resolved at $\bar{\Gamma}$ and $\bar{J}$. Since S_3 and S'_3 degenerate at $\bar{\Gamma}$ and $\bar{J}$, it is arbitrary which branch corresponds to the S'_3 band between $\bar{\Gamma}$ and $\bar{J}$. S_1 and S_2 are even for both mirror axes, and S'_2 is odd for both axes. The symmetries of the two branches of S_3 are also opposite to each other in $\bar{\Gamma}$-$\bar{J}$, but not so clear in $\bar{\Gamma}$-$\bar{J}'$.

Besides the five SS's summarized above, two other spectral features were observed inside the projected bulk band gap. In Fig. 3, we can see a state, denoted as S, around $\bar{\Gamma}_{11}$ at $E_B=\sim2.5$ eV. This state can also be identified in the scan along $\bar{J}_{01}$-$\bar{\Gamma}_{11}$ and $\bar{K}_{00}$-$\bar{\Gamma}_{11}$, at almost the same E_B. S disperses to larger E_B from $\bar{\Gamma}_{11}$, and enters the bulk band region toward $\bar{J}_{01}$, $\bar{J}'_{10}$, and $\bar{K}_{00}$. In addition, a sharply dispersing spectral feature (called S') can be noted around $\bar{J}_{10}$, which crosses the S_3 band and disperses up into the bulk band gap. Though it is possible that some of the spectral features in the bulk-band region are surface resonances, so far we have found five definite SS's and two surface-related states S and S'. These seven states in total will be discussed in Sec. IV.

IV. DISCUSSION

Recently we have identified the dispersions of five SS's for a SD Si(001)2×2-Al surface,[23] which has been known to have essentially the same dimer structure as 2×2-In.[15,22] The result for 2×2-Al is shown in Fig. 7(b) for comparison. In Fig. 7, one can easily see that the two surfaces have five SS bands with very similar E_B's and dispersions. This similarity can be expected from the common surface structure of 2×2-In and -Al and the same valency of In and Al. We note that all SS's of 2×2-In are shifted to smaller E_B by a few tenths of an eV compared to 2×2-Al. However, this shift is not restricted to SS's; the bulk spectral features were also found to shift by about the same amount. Thus the main reason for the shift is the difference in the pinning positions of E_F for the 2×2-Al and -In surfaces.

The surface electronic structures of SD Si(001)2×2-Ga (Ref. 11) and DD Si(001)2×2-In (Ref. 12) have been studied using a rare-gas discharge lamp for parts of the SBZ. These previous results are also shown in Fig. 7(b) for com-

parison: open and filled squares (circles) for 2×2-Ga (-In). The open and filled symbols represent the data points taken at different parts (though symmetrically equivalent) of the SBZ. Along [110] axis ($\bar{\Gamma}$-J) of 2×2-Ga, three SS's were identified, whose E_B's and dispersions are almost the same as those observed for S_1, S_2, and S_3 of 2×2-Al and -In. The splittings of S_2 and S_3 were not observed like for 2×2-Al. For the case of the [$\bar{1}\bar{1}0$] axis ($\bar{\Gamma}$-J'), Enta, Suzuki, and Kono[11] could not draw out the dispersions of S_2 and S_3 because these two SS's appeared not to follow the expected symmetry of the 2×2 SBZ. In comparison with our experimental results for 2×2-Al and -In, the existence of additional branches for S_2 and S_3 along [$\bar{1}\bar{1}0$] ($\bar{\Gamma}$-J') is also apparent for 2×2-Ga (filled squares in the figure). We can easily see that the puzzling nonsymmetric dispersions of S_2 and S_3 observed by Enta, Suzuki, and Kono is due to the existence of these additional branches. That is, it seems that for a part of the scan S_2 and S_3' were dominant [open squares in Fig. 7(b)], but for the other part of the scan only S_2' and S_3 appeared (filled squares). In fact, S_2' and S_3' were hardly observed along [$\bar{1}\bar{1}0$] in our works for 2×2-Al and -In due to their odd-symmetry properties. The appearance of all the branches of S_2 and S_3 along [$\bar{1}\bar{1}0$] for 2×2-Ga can, then, be explained by the fact that the experiment for 2×2-Ga was done with *unpolarized* light from a He discharge lamp.

For 2×2-In, Northrup *et al.*[12] and Karlsson[27] reported ARPES spectra on a DD surface along the [010] axis ($\bar{\Gamma}$-$\bar{K}$) to identify three SS's [the circles in Fig. 7(b)]. This result agrees quite well with the present result for SD 2×2-In if the whole states are shifted by $\sim$0.1 eV to smaller E_B. This shift can be ascribed to the difference in the pinning positions of E_F, which is confirmed by concomitant shifts of the bulk features.[27] The dispersions of the first and second SS bands of Refs. 12 and 27 are almost identical to those of S_1 and S_2'. This comparison makes it possible to understand the appearance of a SS around $\bar{\Gamma}_{00}$ below S_1 (closed circles) as part of the S_2 band, which was not interpreted before.[12] It seems that the splitting of S_3 was not noticed by Northrup *et al.*, which is also almost the case for the present study due to the broad width and weak intensity of S_3 along [010]. Comparing the raw spectra for the previous[27] and present experiments, we could see that the spectral features of the previous work are much broader than the present work, which can be the reason Northrup *et al.* could not resolve the two branches of S_2 and S_3.

From the arguments given above, it is clear that our results for In and Al can be interpreted consistently and further resolve the puzzling spectral features of the previous ARPES results for 2×2-Ga (Ref. 11) and -In.[12] For group-III metals Al, Ga, and In, the similarity of the surface electronic structures of the 2×2 phases is remarkable. This sort of similarity of the surface electronic structures of different adsorbates with the same valency and close surface structures has been well established for group-III metal adsorption on Si(111) (Refs. 1 and 28) and alkali-metal adsorbates on Si(001).[1,4,5]

The obtained dispersions for 2×2-In are also compared to those calculated by Northrup *et al.*[12] along [010] [filled circles of Fig. 7(a)]. The calculated data in Fig. 7(a) were shifted by $\sim$0.1 eV for better agreement. Though Northrup *et al.* interpreted their result as only three SS bands, it seems that there exist at least four SS bands. It comes from the noticeable discontinuity of the second band at $\sim$1.2 eV in the middle of $\bar{\Gamma}$-$\bar{K}$, which cannot be connected as one band. Except for the absence of S_3' in the calculation and the discrepancy in a part of the dispersion of S_2, the agreement between the calculation and our result is quite reasonable. Therefore, we can claim that our result is not in contradiction with this calculation.

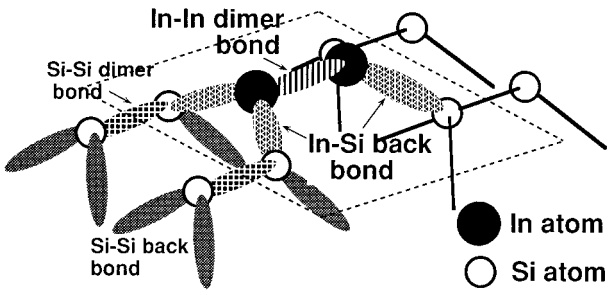

FIG. 8. Schematic illustration of atoms and bonds in a 2×2 unit cell (dashed lines) for the structure model of Si(001)2×2-In given in Fig. 1(b).

The structure models for 2×2 phases of Al, Ga, and In (Refs. 10, 12, 15, and 22) consist of two Si dimers and one metal-dimer in a surface unit cell [Fig. 1(b)]. These structures have ten surface electrons in each surface unit cell, six from two metal atoms (s^2p) and four from the otherwise dangling bonds of Si dimers. One can expect from this structure that the surface electrons form five bonds in each unit cell: four back bonds between four Si dimers and an adsorbate dimer, and one dimer bond within the adsorbate dimer. This bonding configuration is depicted schematically in Fig. 8. In this picture, the covalent bonding between Si and the adsorbate and within adsorbate dimer atoms are assumed. Recent *ab initio* calculations support this bonding configuration as well as the parallel dimer structure:[13,14,18] for Ga (Ref. 18) and Al (Refs. 13 and 14), the calculations have shown that there is indeed well-localized bond charges not only between Si and the adsorbate but within the adsorbate dimer atoms. Concerning the SS bands, the aforementioned bonding configuration results in five fully occupied SS bands at most, and thus the semiconducting surface: one SS from the adsorbate dimer bond and four from the four back bonds. Besides these five SS's, one can also expect SS's or surface resonances due to the dimer and back bonds of substrate Si dimers.

This picture agrees very well with the existence and dispersions of the five intrinsic SS's observed within the bulk-band gap in the present work as follows. On a clean Si(001) 2×1 surface, the Si dimer-bond and Si-Si back-bond SS's (see Fig. 8) (denoted as subsurface SS's), are located below $E_B=\sim$2.0 eV at least along [$\bar{1}\bar{1}0$] and [010].[1,26] Moreover, since the 2×2 surface are stabilized by saturation of dangling bonds, the E_B's of the subsurface SS's of 2×2-In are expected to become larger than the values on the clean Si(001) surface. This argument is verified by identifying the subsurface SS's on the 2×2-In surface at E_B's considerably larger than those found for the clean Si(001) surface,[26] which

will be shown below. Thus the only possible SS's in the band-gap region above $E_B = 2.0$ eV are SS's due to bonds between Si and the adsorbate, and within adsorbates. From these facts, it is unambiguous to assign the five SS's as the dimer- and back-bond SS's of the adsorbate dimers. The possibility of surface umklapp process as the origin for any of the five SS's are ruled out, since almost all of their bands were identified throughout the SBZ and no corresponding bulk spectral features were observed at the same E_B.

For further assignments of the origin of each SS, the details of the dispersions and symmetry properties should be considered. The four identical back-bond orbitals are degenerated if there is no interaction between them. However the SS's from the back bonds may split into several bands, through possible interaction between them like the π bonding between the dangling bonds of Si dimers[1,26,29] and the lone pairs of As dimers[1–3] on Si(001). Thus, from the two branch structures and degeneracies of S_2 (S_2') and S_3 (S_3') observed, it is tempting to assign these four larger E_B SS's to the four back-bond SS's and thus automatically the remaining state S_1 as the adsorbate dimer-bond SS. The SS due to adsorbate dimer bond is expected to have smaller E_B than the back-bond SS, since the electronegativity difference of the metal adsorbate and Si would cause a stronger binding between Si and the metal adsorbate than between adsorbate atoms.

Recently, Yamazaki *et al.*[20] have studied the details of the surface electronic structure of the Al-induced 2×2 and 2×3 surfaces by an *ab initio* molecular-dynamics method. If we compare the calculated local density of states (LDOS) on an Al and a Si dimer atom of the parallel dimer structure,[20] it is evident that the Al dimer-bond SS is located at smaller E_B than the back-bond SS's. In addition, the LDOS on the Si dimer atom bonded to the Al dimer suggests two important natures of the back-bond SS's.[20] First the back-bond SS's appears to have larger E_B than that of the dangling-bond SS of clean Si(001)2×1. This is natural because the dangling-bond SS's are saturated by bonding with Al in 2×2-Al. Second, these back-bond SS's are stabilized by forming π bonds between them.[20] Therefore, the back-bond SS's are expected to have E_B's greater than those of the dangling-bond SS's, ~1 eV, and π symmetry. Similar π symmetry for dangling bonds saturated by metal adsorbates has been established theoretically and experimentally for alkali-metal adsorption on Si(001).[4,5] These results strongly support our assignment for the SS's observed for 2×2-Al and -In as follows. First, the E_B's of dimer- and back-bond SS's estimated above rule out the possibility of assigning S_1 as a back-bond SS. Second, since the four back-bond SS's are expected to have π bonding between them, two of them should have even symmetry and the others odd for a given mirror axis. This is indeed the case in our result for S_2, S_2', S_3, and S_3' of 2×2-In at least along [110] as shown in Fig. 7(a). Since the dimer bond is a σ bonding, the SS due to the dimer bond should be even for both mirror axes, which is in agreement with the observed symmetry property of S_1.

In addition to the assignments of the origins of observed SS's, we can also deduce an important conclusion concerning the surface structure of the 2×2 phase from a comparison with the theoretical calculation. In the above theoretical report,[20] the LDOS for the two structural models, the parallel and orthogonal dimer models, are also compared. In the orthogonal dimer model, the states localized on the Al dimers are located around E_F, to result in a metallic surface or at least a very small band gap, while the parallel dimer model results in a semiconducting surface with a clear band gap. This obvious difference in the calculated surface electron structures near E_F rules out the possibility of the orthogonal dimer model, since our result shows that the 2×2 surfaces are semiconducting, with the band gaps larger than 0.6 eV for both 2×2-Al and -In.

The 2×2 surfaces have recently been investigated in detail by STM.[10,17,19] These STM studies for 2×2-Ga (Ref. 12) and -In (Ref. 19) have shown clear images of an occupied state at a bias voltage of ~2.0 eV. From the shape of these images and theoretical calculations,[14,14,20] these images can be interpreted as due mainly to the back-bond SS's. This interpretation is consistent to our ARPES result observing back-bond SS's between 1 and 2.2 eV in E_B. Another STM work reported similar occupied-state images at a bias voltage of ~3.2 eV for 2×2-Al.[17] This bias voltage was further interpreted as E_B's, the back-bond SS's in disagreement with our ARPES measurements. Since the STM image is a result of the integrated density of states between E_F and the bias voltage, the bias voltage of the STM image cannot be directly related to the E_B's of the SS's. Hence the spectroscopic interpretation of the STM image for 2×2-Al (Ref. 17) seems inappropriate, though the result itself is not in contradiction with our ARPES result.

Other than the aforementioned five SS's, another dispersing state (S) was found around $\bar{\Gamma}_{11}$ at ~2.5 eV, which is well inside the bulk band gap. The same state could be observed for Si(001)2×2-Al, though its intensity was very weak. Based on the discussion given above, S may be attributed to a back-bond or a dimer-bond SS of subsurface Si dimers. In fact, a very similar SS has been found on clean Si(001) surface around the same $k_\parallel$ with $E_B = \sim2.0$ eV.[26] This indicates that these two SS's have a similar origin. It was noted that this state on clean Si(001) could be interpreted as the dimer-bond SS of Si dimers or as a bulk band caused through the surface umklapp process.[1,26] The interpretation by surface umklapp process for S is also possible because the surface umklapp condition for 2×2 includes that for 2×1. A state similar to the sharply dispersing state S' around J_{10} mentioned above has also been observed on the clean Si(001) surface with the same dispersions, but at smaller E_B than S'. The origin of this state has been uncertain.[1,26] S' appeared not to follow the symmetry of the 2×2 SBZ. From the above comparison to the clean Si(001) surface, it can be concluded that S and S' are related not to In adsorbates but to the Si atoms in the subsurface region; thus they are subsurface SS's. We also note that, for 2×2-In, S and S' are shifted to larger E_B by the same amount (~0.5 eV) from their E_B on clean Si(001).[26] Since no concomitant shifts of the bulk features are noticed, the shift should be attributed to the stabilization of the surface through the saturation of the dangling bonds by adsorption of In. This observation confirms the argument given above that there can be no subsurface related SS's above $E_B = \sim2.0$ eV for the 2×2-In surfaces.

V. CONCLUSIONS

An ARPES study using synchrotron radiation has been done in order to elucidate the electronic structure of a SD Si(001)2×2-In surface. Through detailed ARPES measurements for seven different symmetric lines in the SBZ—[110], $[\bar{1}\bar{1}0]$,[010], $\bar{\Gamma}_{10}$-$\bar{\Gamma}_{11}$, $\bar{\Gamma}_{01}$-$\bar{\Gamma}_{11}$, $\bar{J}'_{00}$-$\bar{J}'_{10}$, and $\bar{J}_{00}$-$\bar{J}_{01}$—we have identified the dispersions of five SS bands, one (S_1) less than 1 eV and the others (S_2, S'_2, S_3, and S'_3) between 1 and ~2.2 eV in E_B. It is also clearly shown that this surface is semiconducting with no spectral features between E_F and ~0.6 eV in E_B. The SS nature of the five observed bands was confirmed by their presence inside the bulk band gap and the $h\nu$ independence of their E_B and dispersions. This observation confirms our previous results for the 2×2-Al surface,[23] and can be consistently interpreted with previous ARPES studies on Si(001)2×2-Ga (Ref. 11) and -In.[12]

These ARPES results for 2×2-Al (Ref. 23) and the present 2×2-In unambiguously distinguishes the two proposed structure models of the 2×2 phase—the orthogonal and parallel dimer models[10,12,15]—when we compare the experimental results with the *ab initio* calculation,[20] which predicted a clear semiconducting surface for the parallel dimer model and a metallic surface for the orthogonal dimer model.

Besides the dispersions, the symmetries of the SS's with respect to the two mirror axes of the 2×2 phase were determined using the linear polarization of synchrotron radiation. S_1 and S_2 are even for both mirror axes, and S'_2 is odd for both axes. The symmetries of the two branches of S_3 are opposite along [110], but not clear along $[\bar{1}\bar{1}0]$. From the characteristics of the dispersions and symmetries, it is assumed that S_1 is due to the In-In dimer bond and S_2 (S'_2) and S_3 (S'_3) to the In-Si back bonds of the In dimers. This assignment reinforces the similar suggestion for 2×2-Al (Ref. 23) and is supported by a recent *ab initio* calculation.[20]

Other than the five SS bands mentioned above, we have identified two other spectral features S and S' in the bulk band gap around $\bar{\Gamma}_{11}$ and $\bar{J}_{10}$, respectively, which are attributed to subsurface SS-related Si dimers because of a close resemblance to the electronic structures of the clean Si(001) surface.[1,26]

ACKNOWLEDGMENTS

The authors are grateful to Dr. K. Sakamoto and Dr. T. Sakamoto for providing a well-oriented Si wafer, and to A. Harasawa for technical support at PF. They also thank Dr. Y. Yamazaki for sending them his calculation result, and to Professor A. Kawazu for valuable discussions. This work was performed under the Photon Factory Proposal No. 94-G189.

[1] For a review, see R. I. G. Uhrberg and G. V. Hansson, Crit. Rev. Solid State Mater. Sci. **17**, 133 (1991).

[2] R. D. Bringans, in *Angle-Resolved Photoemission*, edited by S. D. Kevan (Elsevier Science, Amsterdam, 1992).

[3] R. I. G. Uhrberg, R. D. Brigans, R. Z. Bachrach, and J. E. Northrup, Phys. Rev. Lett. **56**, 520 (1986); J. Vac. Sci. Technol. A **4**, 1259 (1986).

[4] T. Abukawa, T. Kashiwakura, T. Okane, Y. Sasaki, H. Takahashi, Y. Enta, S. Suzuki, S. Kono, S. Sato, T. Kinoshita, A. Kakizaki, T. Ishii, C. Y. Park, S. W. Yu, K. Sakamoto, and T. Sakamoto, Surf. Sci. **261**, 217 (1992), and references therein.

[5] T. Abukawa, T. Kashiwakura, T. Okane, H. Takahashi, S. Suzuki, S. Kono, S. Sato, T. Kinoshita, A. Kakizaki, T. Ishii, C. Y. Park, K. A. Kang, K. Sakamoto, and T. Sakamoto, Surf. Sci. **303**, 146 (1994), and references therein.

[6] T. Sakamoto and H. Kawanami, Surf. Sci. **111**, 177 (1981).

[7] J. Knall, J.-E. Sundgren, G. V. Hansson, and J. E. Greene, Surf. Sci. **166**, 512 (1986).

[8] B. Bourguignon, K. L. Carleton, and S. R. Leone, Surf. Sci. **204**, 455 (1988).

[9] T. Ide, T. Nishimori, and T. Ichinokawa, Surf. Sci. **209**, 335 (1989).

[10] J. Nogami, A. A. Baski, and C. F. Quate, Phys. Rev. B **44**, 295 (1991), and references therein; A. A. Baski, J. Nogami, and C. F. Quate, J. Vac. Sci. Technol. A **8**, 245 (1990).

[11] Y. Enta, S. Suzuki, and S. Kono, Surf. Sci. **242**, 277 (1991); Y. Enta, Ph.D. thesis, Tohoku University, Japan, 1990.

[12] J. E. Northrup, M. C. Schabel, C. J. Karlsson, and R. I. G. Uhrberg, Phys. Rev. B **44**, 13 799 (1991).

[13] G. B. Adams and O. F. Sankey, J. Vac. Sci. Technol. A **10**, 2046 (1992).

[14] G. Brocks, P. J. Kelly, and R. Car, Phys. Rev. Lett. **70**, 2786 (1993).

[15] H. Sakama, K. Murakami, K. Nishikata, and A. Kawazu, Phys. Rev. B **48**, 5278 (1993); **50**, 14 977 (1994); and (private communication).

[16] B. E. Steele, L. Li, J. L. Stevens, and I. S. T. Tsong, Phys. Rev. B **47**, 9925 (1993).

[17] H. Itoh, J. Itoh, A. Schimid, and T. Ichinokawa, Phys. Rev. B **48**, 14 663 (1993); Surf. Sci. **302**, 295 (1994).

[18] Y. Qian, M. J. Bedzyk, S. Tang, A. J. Freeman, and G. E. Franklin, Phys. Rev. Lett. **73**, 1521 (1994); S. Tang, A. J. Freeman, Y. Qian, G. E. Franklin, and M. J. Bedzyk, Phys. Rev. B **51**, 1593 (1995).

[19] C. Zhu, T. Hayashi, S. Misawa, and T. Tsukahara, Jpn. J. Appl. Phys. **33**, 3706 (1994).

[20] Y. Yamazaki, M. Ikeda, Y. Morikawa, and K. Terakura, in *Interface Control of Electrical, Chemical and Mechanical Properties*, edited by S. P. Murorka, T. Ohmi, K. Rose, and T. Seidel, MRS Symposia Proceedings No. 318 (Materials Research Society, Pittsburgh, 1994), p. 257.

[21] H. W. Yeom, T. Abukawa, M. Nakamura, S. Suzuki, S. Sato, K. Sakamoto, T. Sakamoto, and S. Kono, Surf. Sci. (to be published).

[22] H. W. Yeom, T. Abukawa, M. Nakamura, X. Chen, S. Suzuki, S. Sato, K. Sakamoto, T. Sakamoto, and S. Kono, Surf. Sci. Lett. (to be published).

[23] H. W. Yeom, T. Abukawa, Y. Takakuwa, M. Nakamura, M. Kimura, A. Kakizaki, and S. Kono, Surf. Sci. Lett. **321**, L177 (1994).

[24] A. Ishizaka and Y. Shiraki, J. Electrochem. Soc. **113**, 666 (1986).

[25] T. Abukawa, M. Sasaki, F. Hisamatsu, T. Goto, T. Kinoshita, A.

Kakizaki, and S. Kono, Surf. Sci. **325**, 33 (1995).
[26] L. S. O. Johansson, R. I. G. Uhrberg, P. Märtensson, and G. V. Hansson, Phys. Rev. B **42**, 1305 (1990), and references therein.
[27] C. J. Karlsson, Ph.D. thesis, Linköping Institute of Technology, Sweden, 1994.
[28] T. Kinoshita, S. Kono, and T. Sagawa, Phys. Rev. B **34**, 3011 (1986).
[29] P. Kruger and J. Pollman, Phys. Rev. B **38**, 10 578 (1988); Z. Zhu, N. Shima, and M. Tsukada, *ibid.* **40**, 11 868 (1989).